Applied Surface Science 591 (2022) 153209
https://doi.org/10.1016/j.apsusc.2022.153209

Reactive Molecular Dynamics Simulations of Thermal and Shear-Driven Oligomerization

Fakhrul H. Bhuiyan[1], Seong H. Kim[2], Ashlie Martini[1]

[1]Department of Mechanical Engineering, University of California Merced, 5200 N. Lake Road, Merced, California 95343, United States

[2]Department of Chemical Engineering and Materials Research Institute, Pennsylvania State University, University Park, Pennsylvania 16802, United States

Abstract

Mechanochemical reactions play a critical role in many manufacturing, tribological, and synthesis processes. Often, these reactions happen at a sliding interface which makes them difficult to study experimentally. Such reactions are not fully understood since the reactant species are subject to frictional heating and mechanical stress simultaneously. Here, reaction pathways driven by heat, normal stress, and shear stress were investigated using reactive molecular dynamics simulations of mechanochemical oligomerization of α-pinene molecules on silica. Results identified shear stress as the key driver of oligomerization reactions under tribological conditions. Normal stress alone was ineffective in inducing any reactions and oligomerization could be driven thermally only at very high temperatures. Analysis of the reaction pathways showed that shear can activate multiple reaction mechanisms that are not accessible thermally. Calculations of bond lengths and dihedral angles revealed that such activations are associated or accompanied with physical deformation of reacting species. The findings from reactive molecular dynamics simulations

provide critical insights into the activation mechanisms underlying mechanochemical reactions that can guide design of materials and processes with optimized and potentially tunable shear-induced reactions.

Keywords

Reactive Molecular Dynamics; Mechanochemical reaction; Tribochemistry; Shear-driven reaction; Oligomerization

1. Introduction

Mechanochemistry refers to chemical reactions that are promoted or facilitated by mechanical stress. Such mechanochemical reactions have enabled exciting new alternatives to conventional manufacturing and synthesis technologies that are simpler, faster, and greener [1,2]. Mechanochemical processes are also relevant to the field of tribology since stress-induced reactions enable anti-wear lubricant additives to form protective films on the surfaces of mechanical components during operation [3–5]. These protective layers, also known as tribofilms, are critically important for function and durability of machine components because they reduce wear and friction. However, the mechanisms underlying tribofilm formation are not fully understood because of the complexity and dynamic nature of the interfacial conditions, which are continuously evolving during sliding. Further, at a sliding interface, heat, normal stress, and shear stress are present, any or all of which can drive chemical reactions. Differentiating the contributions of heat, normal stress, and shear stress to tribofilm formation is critical to understanding this complex and important process.

Macroscopic experiments have been used to understand the effect of different possible contributions on tribofilm formation. A study on dimethyl-disulfide in a sliding copper-copper interface showed that tribofilms formed with negligible interfacial temperature rise, which indicated that the reactions leading to tribofilm formation were stress-induced [6]. The effect of stress has been studied using the stress-augmented thermal activation model, also known as the Bell model [7], for many different systems. Using this theory, wear of diamond-nanoparticle-containing amorphous carbon films sliding against Al_2O_3 was shown to be stress-induced since the wear rate increased exponentially with contact pressure [8]. Another study on the decomposition of adsorbed methyl thiolate species on copper in ultrahigh vacuum calculated the

force required for mechanochemical reactions [9]. Measurements of film growth during lubrication experiments enabled differentiation between the effects of normal and shear stress. One such experiment with zinc dialkyldithiophosphate (ZDDP) on tungsten carbide showed that the rate of tribofilm formation had an exponential dependance on shear stress rather than normal stress [10]. A similar dependance was also observed on steel surfaces [11]. A study on corrosion resistant phosphate coatings showed that tribofilms consisting of manganese phosphate formed on the uncoated counter-surface and the formation was shear induced [12].

Polymerization reactions of simple organic molecules at a sliding interface in vapor phase lubrication (VPL) have been studied to explore how shear stress increases the reactivity of chemical species. Ball-on-flat experiments on allyl alcohol, α-pinene, pinane, and n-decane showed that polymerization was shear stress activated and that the internal strain of the molecules played a critical role in the mechanochemical activation [13–15]. The morphological and compositional characteristics of the tribofilms formed by different additives and organic molecules have also been analyzed in macroscopic experiments [16–21]. These studies showed that tribofilm formation relies on the adsorption of additive molecules to the surface and the chemical composition of tribofilms is sensitive to surface chemistry as well. However, macroscale experiments are usually conducted in conditions where measuring the local temperature and stress is quite challenging. In addition, how shear stress promotes the tribochemical reactions is not clear and the effects of heat and shear stress cannot easily be differentiated.

Atomic force microscopy (AFM) has been used to overcome the drawbacks of macroscale experiments by enabling measurement of tribofilm formation at the single-asperity scale. AFM was used as an in-situ tool to show that the trends exhibited by the ZDDP tribofilm growth rate on both Fe-coated and uncoated substrates were consistent with the Bell model predictions [22]. Similar tribofilm growth from ZDDP was observed on aluminum-based interfaces which further demonstrated the role of stress-augmented thermal activation in tribofilm formation [23]. Another AFM single-asperity compression experiment measuring the decomposition of methyl thiolate on Cu surface showed that the reaction rate increased exponentially with normal stress [24]. This finding enabled the development of analytical models for the mechanochemical reaction kinetics.

AFM has also been used to study atomic scale wear phenomena and how stress at sliding interfaces affects material removal from a surface. AFM combined with transmission electron microscopy

was used as an in-situ technique to study the wear of silicon against diamond [25]. The wear of silicon was consistent with an atomic attrition mechanism where the rate of atom removal increased exponentially with contact stress, as predicted by a stress-assisted chemical reaction kinetics model. Another AFM based in-situ experiment studied the influence of shear stress and rubbing time on removal of different functional groups from graphene and found that the reduction in friction due to oxygen removal was consistent with the Bell model [26]. In a subsequent study, bonding between a silica tip and a graphene oxide was modeled as a thermally activated process driven by normal stress while the velocity-dependent wear behavior was explained by shear-driven oxygen removal from graphene [27].

AFM experiments on diamond-like carbon (DLC) showed that the running-in period before achieving superlubricity consisted of removal of the native oxide layer followed by structural ordering to form a graphitic-layered transfer film [28], consistent with the findings from the ball-on-flat testing [29]. The removal of the oxide layer was explained by the Bell model while the structural ordering transformation was explained by a modified Bell model. Wear of amorphous hydrogenated DLC film (a-C:H) was studied using intermittent contact mode AFM to show that wear of a-C:H was consistent with a stress-assisted reaction rate theory as the rate of atom removal increased exponentially with contact stress [30]. Since there was no sliding involved in this mode of AFM, the contribution of normal stress alone could be studied. Investigations of atomic scale wear processes using AFM were also carried out on polymeric surfaces, NaCl step edges, and single crystal calcite edges to show that wear was a thermally activated, stress-assisted process [31–33]. However, AFM experiments cannot show how shear stress activates chemical species at an interface nor provide a complete description of the different contributions of normal and shear stress. Further, the rubbing motion of the tip on a substrate can cause a local rise in temperature which cannot be measured directly.

Although experiments at different length scales have demonstrated the role of stress in tribofilm formation, they have not been able to directly differentiate the contributions of heat, normal stress, and shear stress. Therefore, such experiments are often complemented by computational methods that can be used to elucidate experimental findings or to test different hypotheses. The use of computational methods, such as first principles calculations and molecular dynamics (MD)

simulations, can provide information about reactions between two surfaces that is not accessible in experiments.

First principles calculations can accurately capture the atomic behavior of a system, and thus, quantum mechanics/molecular mechanics (QM/MM) simulations, ab initio calculations, and density functional theory (DFT) calculations have been used extensively to study mechanochemical reactions involved in tribofilm formation. QM/MM dynamic simulations were used to evaluate different dissociation mechanisms of molybdenum dithiocarbamates molecule at an Fe interface [34]. The study showed how oxygen atoms in the ligand position of the additive molecule and the metallic interface could alter the dissociation mechanism. Ab initio calculations identified the reaction pathway and associated energy barrier for adsorption of trimethyl-phosphite on Fe(110), and suggested that dissociative adsorption was energetically more favorable than molecular adsorption [35]. A subsequent first principles-based study showed that, at lower loads, the longer hydrocarbon chains tributyl phosphite could keep the surfaces farther apart than trimethyl phosphite [36]. DFT was used to calculate the activation energy for stress-assisted decomposition of methyl thiolate adsorbed on Cu(100) surface consistent with the experimentally calculated activation energies following the Bell model [24]. Another DFT study investigated three different reaction mechanisms of tricresyl phosphate decomposition on Fe(110) surface and showed that all three mechanisms could be thermally accessible [37]. DFT was used to develop a set of theoretical rules that successfully predicted the chemical behavior of several diatomic molecules when the molecules were stretched by an external mechanical force [38]. DFT-calculated reaction energy of siloxane bond formation at a silanol terminated silica interface suggested that the elastic deformation of the near-surface bulk region surrounding the contact could make significant contributions to the mechanochemical response of the system [39].

Generally, most first principles-based studies only considered one or a few molecules with restricted dynamics since the calculations are extremely computationally expensive. DFT calculations involve no dynamics at all, and thus, cannot be used to study the dynamic evolution of a system. Some of these limitations can be circumvented using MD simulations. The development of reactive force fields such as ReaxFF has allowed MD simulations to study the chemical reactions of a wide range of complex tribological systems [40]. ReaxFF was initially

developed to study hydrocarbon reactivity but later extended to a wide array of systems, including mechanochemical reactions at tribological interfaces [41].

ReaxFF simulations have been used to study tribochemical wear from surfaces. ReaxFF studies on material removal from silica or silicon surface with water as a lubricant showed that water could have competing effects on wear [42]. Specifically, water can provide oxygen to the silica surface to form Si-O-Si bonds, which facilitates wear [43,44], but can also minimize contact between the sliding surfaces, which reduces wear mechanically [45,46].

Tribofilm formation mechanisms have also been studied using ReaxFF MD. Recently, an MD simulation of tri(n-butyl)phosphate and tri(s-butyl)phosphate showed that the tribofilm formation can be shear driven [47]. A study on di-tert-butyl disulfide, an extreme pressure additive, on Fe(100) surfaces showed the decomposition pathway of the additive and found that the reaction yield across a range of different temperatures could be described by the Bell model [48,49]. Reactive MD simulations of thermal decomposition of two TCP isomers on Fe_2O_3 and Fe_3O_4 surfaces detected cresol as the main decomposition product, as observed in corresponding experiments [50]. Further, consistent with the experiments, MD simulations demonstrated the relative reactivity of the two isomers and the two surfaces.

Reactive MD simulations complementing experiments in VPL have provided valuable insight on how stress drives tribochemical reactions. ReaxFF simulations of polymerization of allyl alcohol in VPL reproduced the activation volume calculated in the experiments using the Bell model and suggested that triggering such reactions required distortion of the molecules by shear [13]. Reactive simulations also explained experimental observations of α-pinene tribo-polymerization reactions in VPL on stainless steel and silica [15,51]. The simulations identified shear stress, rather than normal stress, as the key factor driving association reactions of α-pinene molecules. A comparable value of activation volume in the experiments and simulations confirmed the relevance of the simulation results.

Despite this progress, at this point, neither experimental nor computational studies have clearly differentiated the contributions of heat, normal stress, and shear stress in stress-augmented thermal reactions. In this work, α-pinene ($C_{10}H_{16}$) molecules on silica surfaces were studied using reactive MD simulation at different interfacial conditions to identify the effects of normal and shear stress,

and heat on the oligomerization reaction. This study focuses on α-pinene because previous experimental work showed oligomerization of α-pinene could be stress assisted [14,15,51]. However, it was not clear if such oligomers can form thermally and, if so, how the thermal and shear-driven reaction pathways differ. To answer these questions, we performed heating simulations, compression simulations, and sliding simulations of α-pinene molecules at a silica-silica interface. The simulation results identified shear stress as the key driver behind oligomerization of α-pinene molecules. Further, three oligomerization reaction pathways were observed under the identical shear condition, and how heat or shear activated each reaction pathway was investigated.

2. Methods

MD simulations of α-pinene molecules between two amorphous silica slabs (Fig. 1) were carried out using the ReaxFF force field [40,52] with a set of parameters previously developed from a combination of parameters for C/H/O [53,54], and Si/C interactions [55]. This force field was used for a similar system in a previous study [15]. All MD simulations were performed using the Large Atomic/Molecular Massively Parallel Simulation (LAMMPS) software [56]. Postprocessing was carried out using in-house python scripts and OVITO software [57].

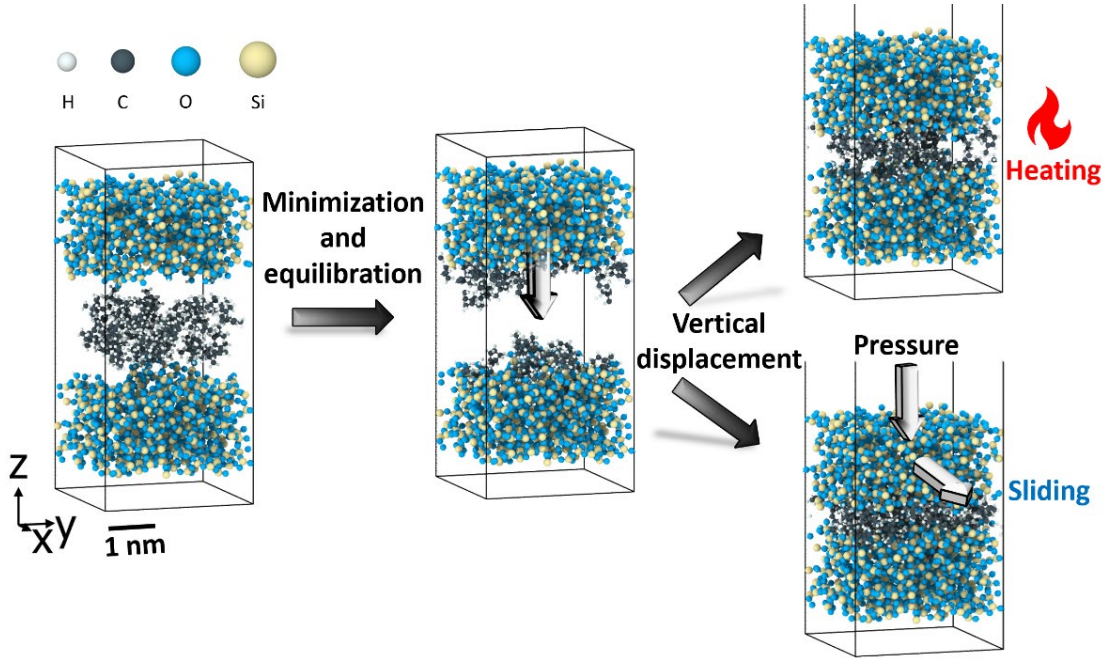

Fig. 1. The simulation model system consisting of α-pinene molecules between amorphous silica slabs. From left to right: system equilibration (energy minimization and vertical displacement of the upper slab), and production simulations with heating or sliding. Production simulation for compression is not shown here. The white, black, blue, and yellow spheres represent H, C, O, and Si atoms respectively.

The amorphous silica slabs were created by a process that involved heating up crystalline cristobalite from 300 K to 4000 K at 0.02 K/fs and then cooling it down to room temperature at 0.02 K/fs cooling rate [15]. The presence of a vacuum on top of the slab during the annealing process produced a rough surface (~2 nm roughness) on each slab. The surfaces were then hydroxylated by introducing water molecules at 500 K. The final amorphous slabs were about 18.5 Å thick. Two such silica slabs were then positioned 22 Å apart, with 35 α-pinene molecules placed between the two slabs. The initial slab-to-slab distance was chosen to minimize interactions between the two slabs, provide enough space for the α-pinene molecules to equilibrate without mechanical stress, and minimize the computational time required to bring the slabs together. The number of α-pinene molecules was chosen to form at least a monolayer on each surface. The silica atoms 13.5 Å or farther from the two surfaces were treated as rigid bodies. The canonical ensemble (NVT) was applied to all other non-rigid atoms. Charge equilibration was performed throughout the simulation. The simulation timestep was 0.25 fs. The initial simulation box dimensions were 32.8 x 31.9 x 71 $Å^3$ with periodic boundary conditions in the x and y directions and fixed boundaries in the z direction.

Each MD simulation started with energy minimization and dynamic equilibration at 300 K. The upper slab was then moved towards the bottom slab in the z-direction until the two slabs were approximately 10 Å apart. After this point, the simulations were divided into three categories: heating simulations, compression simulations, and sliding simulations. For the heating simulations, the two slabs were held fixed at their position and the system was heated from 300 K to 900 K, 1200 K, or 1500 K at 1 K/ps heating rate followed by a 2 ns constant temperature simulation (Fig. 1). The maximum normal stress experienced by the α-pinene molecules in the heating simulations was 0.45 GPa (tensile). For the compression simulations, the slabs were brought together at 300 K until the normal stress reached 1 GPa and the normal stress was maintained at this value for 500 ps. Then the system was subjected to a series of loading and

unloading cycles for 2 ns. Each loading cycle involved the application of 1 GPa to the upper slab followed by an unloading cycle where the stress was relieved by lifting the upper slab and holding it 20 Å away from the lower slab. Finally, the effect of shear stress was studied in sliding simulations, where the upper slab was slid against the lower slab at 10 ms^{-1} sliding speed in the x-direction for 2 ns at 1, 2, 3, or 4 GPa compressive normal stress (Fig. 1).

3. RESULTS AND DISCUSSION

Oxidation of α-pinene at one or more carbon sites by surface oxygen atoms resulted in chemisorption of the molecules to the surface. The number of such oxidized molecules increased with time in all simulations (blue lines in Fig. 2, Fig. S1). At room temperature and without any mechanical stress, fewer than four of the 35 α-pinene molecules were oxidized. Then, either heat or mechanical stress was necessary to drive additional oxidation reactions. When temperature was increased to either 900, 1200, or 1500 K, without any stress, oxidation increased and then reached steady state where the system was at dynamic equilibrium. The number of oxidized molecules at dynamic equilibrium increased with temperature (Fig. 2a, Fig. S1a, Fig. S1b).

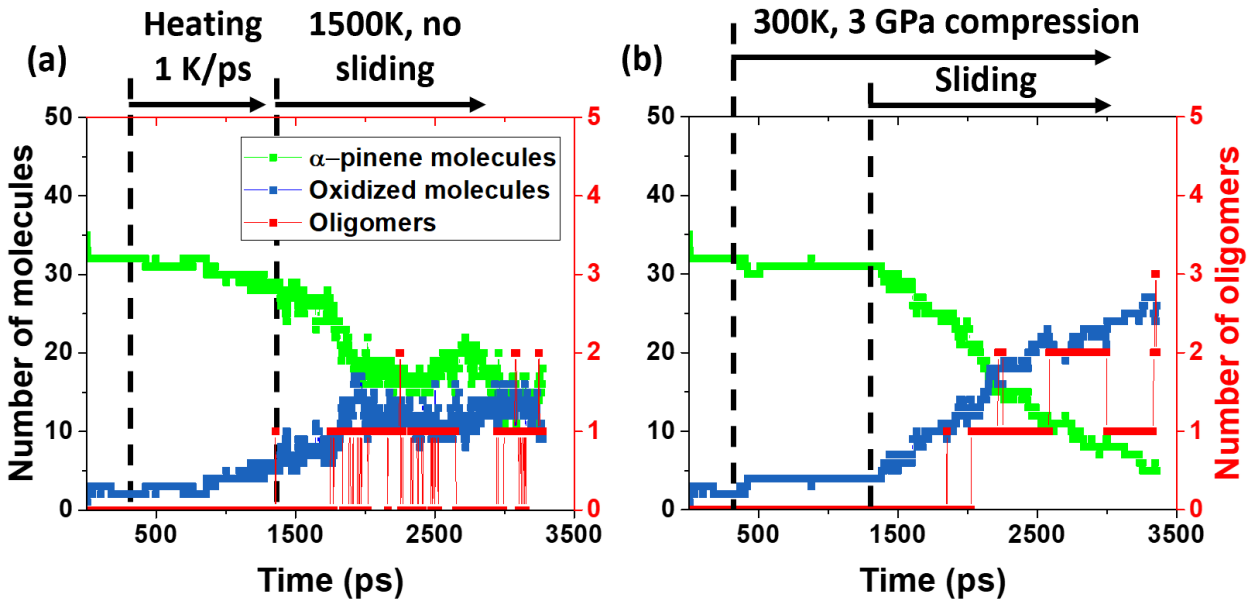

Fig. 2. Evolution of chemical species in simulations at (a) 1500 K without pressure or sliding and (b) room temperature with sliding at 3 GPa. The number of α-pinene and oxidized molecules are plotted in green and blue, respectively, against the left ordinate axis and the number of oligomers is plotted in red against the right ordinate axis.

The effect of normal stress was tested with simulations at room temperature by moving the top slab downwards to apply 1 GPa contact pressure and then lifting it back up to release the pressure in cycles. It was found that, even after four cycles of loading and unloading, only two additional α-pinene molecules were oxidized (Fig. S1c). This indicated normal stress could not efficiently drive these oxidation reactions. However, in sliding simulations, oxidation of α-pinene via reactions with the surface was observed at room temperature under all normal stress conditions. Representative results are shown for 1 GPa (Fig. S1d) and 3 GPa (Fig. 2b). The average shear stresses, calculated from the average friction force on the upper slab and the surface area, increased with applied normal stress (Fig. S2). Of all the simulation conditions tested, the most oxidized molecules were observed in the sliding cases (Fig. 2b, Fig. S1d), suggesting shear stress plays an important role in α-pinene reactivity.

The number of α-pinene molecules after sliding started at each normal stress was fitted to the first order kinetics equation to calculate reaction rate (Fig. S3). The reaction rates were then used to calculate activation volume from the slope of the linear relationship between the natural log of reaction rate and shear stress derived from the Bell model [7]:

$$ln(k) = \tau \frac{\Delta V^*}{K_b T} + \left(ln(A) - \frac{E_a}{K_b T} \right) \quad (1)$$

where, k is reaction rate, τ is shear stress, ΔV* is activation volume, A is the pre-exponential factor, E_a is activation energy, T is temperature, and K_b is the Boltzmann's constant. The calculated activation volume was 4.0±0.3 Å^3 (Fig. S4), which is comparable to previously reported activation volumes for α-pinene (4.2-14.5 Å^3) [5,15]. The details of the activation volume calculation are provided in the supplementary material.

α-pinene is a bicyclic molecule consisting of the highly strained reactive four-membered ring (C2, C3, C3a, and C4) and the six-membered ring that contains the reactive double bond site (C1=C6), see inset to Fig. 3a. The most reactive site on the α-pinene molecule for oxidative chemisorption was identified in each simulation based on the number of oxidation events. An oxidation event was counted the first time a covalent bond formed between a given carbon atom and a surface oxygen atom. Then the percentage of oxidation events at each carbon site relative to the total number was calculated (Fig. 3). Interestingly, different trends were observed from the analyses of simulations with heating and sliding.

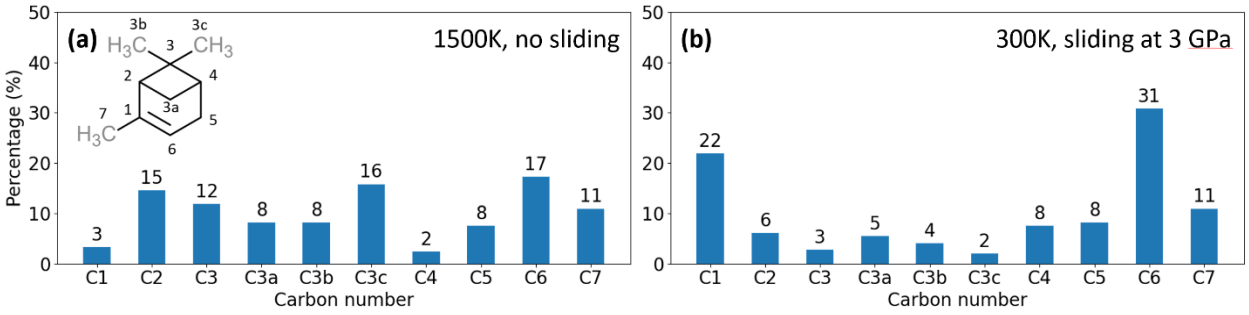

Fig. 3. Percentage of oxidation at different carbon sites compared to all unique C-O bonds formed in simulations at (a) 1500 K without pressure or sliding and (b) room temperature with sliding at 3 GPa. At high temperature, carbon atoms in the four-membered ring were more reactive whereas, in the sliding simulation, carbon atoms at the double bond sites were more reactive.

At 1500K (Fig. 3a), about 60% of the oxidation occurred at the four-membered ring (C2, C3, C3a, C3b, C3c, and C4) while only about 20% occurred at the double bond site (C1 and C6). The same trend was observed at 1200K (Fig. S5b). At 900 K, both the four-membered ring and the double bond sites were oxidized equally (Fig. S5a), but there were very few oxidized molecules (Fig. S1), so the trend was not statistically significant. In the sliding simulations at 300 K, the double bond sites accounted for more than half of the total number of oxidized carbons while the four-membered ring was less reactive with fewer than 30% of the total oxidation (Fig. 3b, Fig. S5c). This indicated that shear stress enabled a reaction mechanism involving the double bond sites that differed from the thermal reaction pathway that involved reactions preferably at the four-membered ring.

Shear stress was also found to play a critical role in oligomerization of α-pinene molecules. Without sliding, oligomers only formed in simulations at 1500 K, the highest temperature tested (Fig. 2, Fig. S1), but not below 1200 K. The average thermal energy of 1200 K corresponds to 0.10 eV; no observation of oligomerization at this temperature means that the high-energy side tail of the Boltzmann distribution is still lower than or not comparable to the thermal activation barrier. In contrast, in sliding simulations, oligomers formed even at 300 K, indicating the barrier was reduced by shear to a level accessible by the high-energy tail of a Boltzmann distribution with an average thermal energy of 0.03 eV. Whether shear stress opened new reaction pathways for

oligomerization or reduced the energy barrier for the same reaction pathway was investigated by studying the oligomerization reaction pathways.

Three oligomerization reaction pathways were found in the simulations, illustrated schematically and with snapshots from the simulations in Fig. 4. Reaction pathway *A* started with oxidative chemisorption of an α-pinene molecule to the surface via one of its carbon atoms. Another α-pinene molecule, which could either be adsorbed to the surface or not, then reacted with the surface oxygen via the double bonded C6 atom in the six-membered ring. At that point, a dimer was formed through an ether linkage with the oxygen originally from the surface.

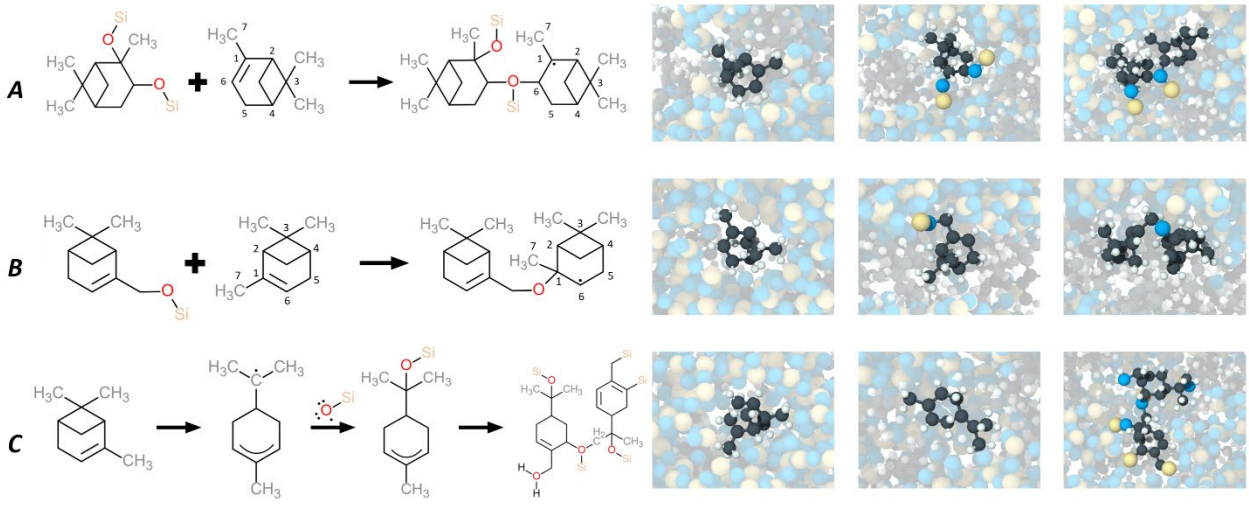

Fig. 4. Representative oligomerization reaction pathways observed in the simulations illustrated schematically on the left and with corresponding snapshots from the simulations on the right. In the schematics, the atoms in the α-pinene molecules are numbered 1 through 6 based on IUPAC nomenclature while the methyl group at C1 is labeled C7 for convenience. In the snapshots, all atoms except those involved in the reaction are faded. Sphere colors are the same as those defined in Fig. 1.

Reaction pathway *B* was initiated in a similar manner by oxidative adsorption of an α-pinene molecule by a surface oxygen. The oligomer was then formed when the surface oxygen reacted with the C1 atom of the double bond site of another α-pinene molecule. So, the double bond site (C1=C6) was activated in both pathways *A* and *B* to form a dimer through an ether linkage. However, in the first reaction pathway, C6 participated in forming the ether linkage whereas in the second reaction pathway, C1 was the participating atom.

Reaction pathway *C* started with opening of the four-membered ring by dissociation of one of the four C-C bonds in that ring. As the four-membered ring opened up, the entire α-pinene molecule was restructured to form an intermediate free radical molecule. This intermediate free radical was then oxidized by the surface. Two of such oxidized species finally reacted with each other to form an oligomer. Note that surface oxygen played a key role in all three reaction pathways. This suggests that environmental oxygen or water molecules may affect polymerization reaction rates, as observed experimentally [58,59]. The effects of oxygen-containing gaseous species on molecular mechanisms could be explored in future simulation-based studies.

Table 1 shows the number of oligomers formed in different simulations via the three reaction pathways. All 5 oligomers observed in the thermal simulation at 1500K were formed only through reaction pathway *C*; in contrast, 8 out of 9 oligomers observed in the sliding simulations were formed via pathways *A* and *B*. This suggests that only reaction pathway *C*, the reaction pathway that activated the four-membered ring (C2, C3, C3a, and C4), is accessible thermally. Shear, on the other hand, not only triggered the thermally accessible reaction pathway at a lower temperature, but also opened two new reaction pathways by activating a different reactive site, namely, the double bond site (C1=C6). Such mechanochemical activation of α-pinene molecule was previously suggested to be the consequence of shear-induced molecular deformation [15].

Table 1. Number of oligomers formed via the three reaction pathways in different simulations.

Reaction pathway	No sliding		Sliding	
	300K 1 GPa	900K – 1500K -	300K 1 GPa	300K 3 GPa
A	0	0	3	1
B	0	0	2	2
C	0	5	0	1

Deformation or structural change of a molecule can be identified just before covalent bond formation from the deviation in bond lengths and angles from their equilibrium values. Bond lengths and angles fluctuate about an equilibrium value and the amplitude and frequency of that fluctuation increase with temperature. The mode of a distribution of lengths or angles for multiple molecules at different times corresponds to the equilibrium value for a given molecular structure.

Then, any persistent change in the length or angle due to distortion of the molecule would be reflected by a shift in the position of the mode or the formation of new peaks in the distribution. Previously, both length and angle histograms were used to investigate distortion of allyl alcohol molecules undergoing mechanically induced association reactions [13].

Equilibrium carbon-carbon bond lengths and dihedral angles were calculated for all α pinene molecules from simulations at 300 K and without any mechanical stress, shown as the black symbols/lines in Fig. 5, Fig. 6, Fig. S6, Fig. S7, and Fig. S8. These equilibrium distributions were then compared with distributions for all non-oxidized reactants in reaction pathways *A* and *B* (Table 1) recorded at 50 different times during the 200 ps just before the ether linkage was formed.

In reaction pathway *A*, one reactant was anchored to the surface while the other reacted with its C6 atom to create the ether linkage (Fig. 4). For the chemisorbed reactant, no consistent changes were observed in the bond length distributions indicating that no deformation occurred before oligomerization (data not shown). This could be explained by the fact that the dimerization reaction (ether linkage formation) occurs at the surface oxygen site to which the α-pinene molecule is anchored. However, the C1C2 and C4C5 bond lengths of the other reactant changed before the reaction, as evidenced by the shift of their respective bond length distributions to the left (Fig. 5). For both bonds, there is a shoulder in the histogram at smaller distances indicating that the bonds were, on average, shorter. None of the other carbon-carbon bond lengths in the six-membered ring (Fig. S6) or any dihedral angles (Fig. S7) exhibited consistent deviations from their equilibrium values before the oligomerization reaction.

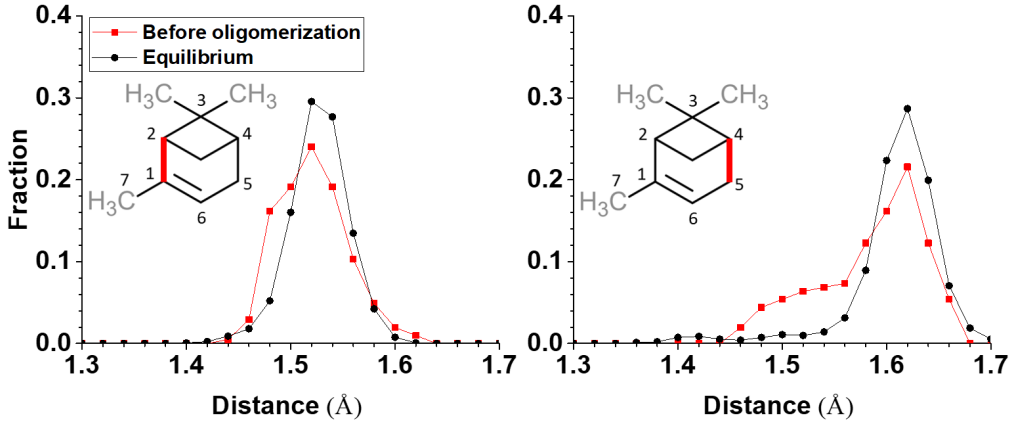

Fig. 5. C1C2 (left) and C4C5 (right) bond length distributions at equilibrium (black) and before oligomerization through reaction pathway *A* (red). The red distributions were calculated over 200 ps before a dimeric species formed and averaged over four α-pinene molecules that were the non-oxidized reactants initially (i.e., reacting with the oxidatively chemisorbed species) in pathway *A*.

In reaction pathway *B*, one reactant was anchored to the surface while the other reacted with its C1 atom to create the ether linkage (Fig. 4). Similar to reaction pathway *A*, the chemisorbed reactants did not show any consistent signs of deformation before oligomerization. However, the C7C1C6C5 dihedral angle distribution before oligomerization was distorted (Fig. 6). Since C1 and C6 are sp^2 hybridized, at equilibrium, C7, C1, C6, and C5 should be in the same plane, making the equilibrium dihedral angle zero. Thus, any change in the dihedral angle suggests out of plane movement of C1 or C5 atom. However, the bond lengths in the six-membered ring closely followed their equilibrium values (Fig. S8), which indicates that the C5 atom remained in plane with C1 and C6. Thus, the distortion in the dihedral angle distribution can be attributed to the C7 atom. As the C7 moved out of the plane, it could in turn affect the hybridization state of the C1 atom, making it more reactive.

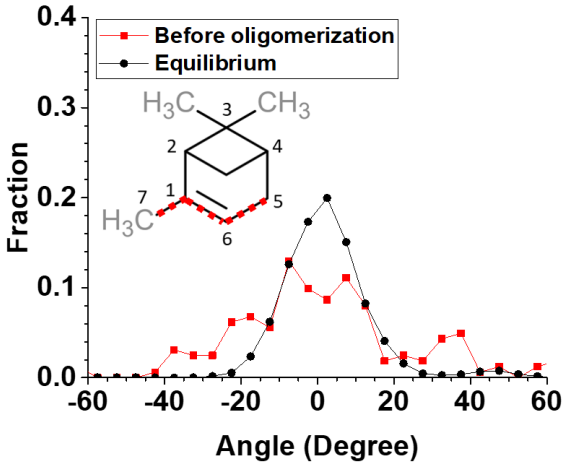

Fig. 6. Comparison between C7C1C6C5 dihedral distributions at equilibrium (black) and before oligomerization through reaction pathway *B* (red). The red distribution was calculated over 200 ps before a dimeric species formed and averaged over four α-pinene molecules that were the non-oxidized reactant initially (i.e., reacting with the oxidatively chemisorbed species) in pathway *B*.

Distributions for reaction pathway *C* were not calculated since only a single oligomer formed via this pathway in the sliding simulations (Table 1). However, this reaction pathway was observed and analyzed previously where it was shown that the reaction was preceded by deformation of the four-membered ring [15]. Thus, for all three pathways, these analyses indicate that shear stress drives chemical reactions by deforming the molecular species to make them more reactive.

4. Conclusion

This work explored the contributions of heat and stress on mechanochemical association reactions forming tribofilms using a bicyclic molecule, α-pinene. At room temperature, both with and without normal stress, the reactivity of α-pinene molecules toward oligomerization was negligible. Reactivity increased with increasing temperature as more α-pinene molecules chemisorbed to the surface. Shear stress, on the other hand, could make the α-pinene molecules reactive even at room temperature and facilitated chemisorption. Analyzing the chemisorbed molecules showed that thermal activation facilitated reactions at the carbon atoms in the four-membered ring of the molecules, whereas shear activation opened reaction pathways at the double bond sites in the six-membered ring. Three oligomerization reaction pathways were found, all of which were readily accessible through shear, but rarely accessible thermally. Bond-by-bond analysis of the α-pinene molecules prior to oligomerization showed that shear caused structural deformation of the molecules from their equilibrium conformations. These results show clearly how heat and shear activate different chemical groups in α-pinene. However, the findings have more general implications for mechanochemical reactions.

First, the findings suggest a physical meaning for the activation volume in mechanochemistry [5]. The Bell model dictates that mechanochemical reactivity should increase exponentially with stress where the exponential stress dependence is related to an activation volume (ΔV^*) needed for the reaction to occur [7]. However, neither the magnitude nor the physical meaning of ΔV^* are fully understood [5]. Some studies compared it with the size of molecules involved in reactions or the unit cell of the substrate, while others suggested it reflects the degree of molecular deformation or deviation from the equilibrium structure [5]. The reactive MD simulation results of this study revealed shear induces reaction pathways that were not accessible in thermal reaction conditions (Table 1). The results also showed that the shear-induced pathways were made available through deformation of reacting molecular species from their equilibrium geometries (Figures 5 and 6).

This suggests that ΔV^* can be interpreted as the propensity of molecules to deform, supporting the hypothesis that activation volume is related to deformation. However, since this study included only one molecule, α-pinene, it cannot provide insight into a possible quantitative physical relationship between deformation and activation volume. Future studies with a homologous series of molecules subject to a range of shear stresses could reveal correlations between the degree of deformation (from the atomic trajectories) and the activation volume (determined from the shear stress dependence).

This study also has implications for reaction selectivity. It is known that, generally, mechanochemical reactions have lower selectivity than thermal reactions [60,61]. In thermal reaction conditions, the pathway with the lowest activation barrier (for example, pathway *C* for α-pinene shown in Fig. 4) can be preferentially accessed by molecules in the high energy tail of the Boltzmann distribution [62]. In mechanochemical conditions, other pathways with higher thermal barriers are activated (as in pathways *A* and *B* in Fig. 4). Depending on the molecular structure and reaction conditions, the lowest barrier pathway can vary. In fact, this is the primary strategy for controlling selectivity in most thermal reactions. In principle, the same should be possible if one knows how the reactant with a specific configuration is activated under what mechanical conditions. The reactive MD study presented here may open such opportunities.

Finally, this study demonstrates the use of reactive MD simulations as a tool for understanding how stress drives chemical reactions. Going forward, this simulation-based approach can be used to suggest ways to tune reactivity through molecular design or manipulation of operating conditions (stress and temperature) to achieve tailorable mechanochemical processes.

Declaration of Competing Interest

The authors declare that they have no known competing financial interests or personal relationships that could have appeared to influence the work reported in this paper.

Acknowledgements

This work was supported by the National Science Foundation (Grant No. CMMI-2038494 and 2038499). The authors thank Arash Khajeh for providing the amorphous silica surfaces used in the simulations and for helpful guidance developing the simulation procedure.

References

[1] J.L. Do, T. Friščić, Mechanochemistry: A Force of Synthesis, ACS Cent. Sci. 3 (2017) 13–19. https://doi.org/10.1021/acscentsci.6b00277.

[2] S. Mateti, M. Mathesh, Z. Liu, T. Tao, T. Ramireddy, A.M. Glushenkov, W. Yang, Y.I. Chen, Mechanochemistry: A force in disguise and conditional effects towards chemical reactions, Chem. Commun. 57 (2021) 1080–1092. https://doi.org/10.1039/D0CC06581A.

[3] H. Spikes, Stress-augmented thermal activation: Tribology feels the force, Friction. 6 (2018) 1–31. https://doi.org/10.1007/s40544-018-0201-2.

[4] W. Tysoe, On Stress-Induced Tribochemical Reaction Rates, Tribol. Lett. 65 (2017) 1-16. https://doi.org/10.1007/s11249-017-0832-x.

[5] A. Martini, S.H. Kim, Activation Volume in Shear-Driven Chemical Reactions, Tribol. Lett. 69 (2021) 1–14. https://doi.org/10.1007/S11249-021-01522-X.

[6] O.J. Furlong, B.P. Miller, P. Kotvis, W.T. Tysoe, Low-temperature, shear-induced tribofilm formation from dimethyl disulfide on copper, ACS Appl. Mater. Interfaces. 3 (2011) 795–800. https://doi.org/10.1021/am101149p.

[7] G.I. Bell, Models for the specific adhesion of cells to cells: a theoretical framework for adhesion mediated by reversible bonds between cell surface molecules, Science. 200 (1978) 618–627. https://doi.org/10.1126/science.347575.

[8] Z. Cao, W. Zhao, A. Liang, J. Zhang, A General Engineering Applicable Superlubricity: Hydrogenated Amorphous Carbon Film Containing Nano Diamond Particles, Adv. Mater. Interfaces. 4 (2017) 1601224. https://doi.org/10.1002/admi.201601224.

[9] H.L. Adams, M.T. Garvey, U.S. Ramasamy, Z. Ye, A. Martini, W.T. Tysoe, Shear induced mechanochemistry: Pushing molecules around, J. Phys. Chem. C. 119 (2015) 7115–7123. https://doi.org/10.1021/jp5121146.

[10] J. Zhang, H. Spikes, On the Mechanism of ZDDP Antiwear Film Formation, Tribol. Lett. 63 (2016) 1-15. https://doi.org/10.1007/s11249-016-0706-7.

[11] J. Zhang, J.P. Ewen, M. Ueda, J.S.S. Wong, H.A. Spikes, Mechanochemistry of Zinc Dialkyldithiophosphate on Steel Surfaces under Elastohydrodynamic Lubrication Conditions, ACS Appl. Mater. Interfaces. 12 (2020) 6662–6676. https://doi.org/10.1021/acsami.9b20059.

[12] D. Ernens, G. Langedijk, P. Smit, M.B. de Rooij, H.R. Pasaribu, D.J. Schipper, Characterization of the Adsorption Mechanism of Manganese Phosphate Conversion Coating Derived Tribofilms, Tribol. Lett. 66 (2018) 1-16. https://doi.org/10.1007/s11249-018-1082-2.

[13] J. Yeon, X. He, A. Martini, S.H. Kim, Mechanochemistry at solid surfaces: Polymerization of adsorbed molecules by mechanical shear at tribological interfaces, ACS Appl. Mater. Interfaces. 9 (2017) 3142–3148. https://doi.org/10.1021/acsami.6b14159.

[14] X. He, S.H. Kim, Mechanochemistry of Physisorbed Molecules at Tribological Interfaces: Molecular Structure Dependence of Tribochemical Polymerization, Langmuir. 33 (2017) 2717–2724. https://doi.org/10.1021/acs.langmuir.6b04028.

[15] A. Khajeh, X. He, J. Yeon, S.H. Kim, A. Martini, Mechanochemical Association Reaction of Interfacial Molecules Driven by Shear, Langmuir. 34 (2018) 5971–5977. https://doi.org/10.1021/acs.langmuir.8b00315.

[16] H. Ma, J. Li, H. Chen, G. Zuo, Y. Yu, T. Ren, Y. Zhao, XPS and XANES characteristics of tribofilms and thermal films generated by two P- and/or S-containing additives in water-based lubricant, Tribol. Int. 42 (2009) 940–945. https://doi.org/10.1016/j.triboint.2009.01.004.

[17] J.F. Luiz, H. Spikes, Tribofilm Formation, Friction and Wear-Reducing Properties of Some Phosphorus-Containing Antiwear Additives, Tribol. Lett. 68 (2020) 1-24. https://doi.org/10.1007/s11249-020-01315-8.

[18] A. Morina, A. Neville, Understanding the composition and low friction tribofilm formation/removal in boundary lubrication, Tribol. Int. 40 (2007) 1696-1704. https://doi.org/10.1016/j.triboint.2007.02.001.

[19] K. Ito, J.M. Martin, C. Minfray, K. Kato, Formation mechanism of a low friction ZDDP tribofilm on iron oxide, Tribol. Trans. 50 (2007) 211–216. https://doi.org/10.1080/10402000701271010.

[20] H. Adams, B.P. Miller, P. V. Kotvis, O.J. Furlong, A. Martini, W.T. Tysoe, In Situ Measurements of Boundary Film Formation Pathways and Kinetics: Dimethyl and Diethyl Disulfide on Copper, Tribol. Lett. 62 (2016) 1-9. https://doi.org/10.1007/s11249-016-0664-0.

[21] M. Rodríguez Ripoll, V. Totolin, C. Gabler, J. Bernardi, I. Minami, Diallyl disulphide as natural organosulphur friction modifier via the in-situ tribo-chemical formation of tungsten disulphide, Appl. Surf. Sci. 428 (2018) 659- 668. https://doi.org/10.1016/j.apsusc.2017.09.100.

[22] N.N. Gosvami, J.A. Bares, F. Mangolini, A.R. Konicek, D.G. Yablon, R.W. Carpick, Mechanisms of antiwear tribofilm growth revealed in situ by single-asperity sliding contacts, Science. 348 (2015) 102-106. https://doi.org/10.1126/science.1258788.

[23] N.N. Gosvami, I. Lahouij, J. Ma, R.W. Carpick, Nanoscale in situ study of ZDDP tribofilm growth at aluminum-based interfaces using atomic force microscopy, Tribol. Int. 143 (2020) 106075. https://doi.org/10.1016/j.triboint.2019.106075.

[24] A. Boscoboinik, D. Olson, H. Adams, N. Hopper, W.T. Tysoe, Measuring and modelling mechanochemical reaction kinetics, Chem. Commun. 56 (2020) 7730-7733. https://doi.org/10.1039/d0cc02992k.

[25] T.D.B. Jacobs, R.W. Carpick, Nanoscale wear as a stress-assisted chemical reaction, Nat. Nanotechnol. 8 (2013) 108-112. https://doi.org/10.1038/nnano.2012.255.

[26] J.R. Felts, A.J. Oyer, S.C. Hernández, K.E. Whitener, J.T. Robinson, S.G. Walton, P.E. Sheehan, Direct mechanochemical cleavage of functional groups from graphene, Nat. Commun. 6 (2015) 1-7. https://doi.org/10.1038/ncomms7467.

[27] S. Raghuraman, P. Boonpuek, K.H. King, Z. Ye, J.R. Felts, The role of speed in atomic scale wear, J. Phys. Chem. C. 125 (2021) 4139-4145. https://doi.org/10.1021/acs.jpcc.0c09191.

[28] K. Wang, J. Zhang, T. Ma, Y. Liu, A. Song, X. Chen, Y. Hu, R.W. Carpick, J. Luo, Unraveling the Friction Evolution Mechanism of Diamond-Like Carbon Film during Nanoscale Running-In Process toward Superlubricity, Small. 17 (2015) 2005607. https://doi.org/10.1002/smll.202005607.

[29] P. Manimunda, A. Al-Azizi, S.H. Kim, R.R. Chromik, Shear-Induced Structural Changes and Origin of Ultralow Friction of Hydrogenated Diamond-like Carbon (DLC) in Dry Environment, ACS Appl. Mater. Interfaces. 9 (2017) 16704–16714. https://doi.org/10.1021/ACSAMI.7B03360.

[30] V. Vahdat, K.E. Ryan, P.L. Keating, Y. Jiang, S.P. Adiga, J.D. Schall, K.T. Turner, J.A. Harrison, R.W. Carpick, Atomic-scale wear of amorphous hydrogenated carbon during intermittent contact: A combined study using experiment, simulation, and theory, ACS Nano. 8 (2014) 7027-7040. https://doi.org/10.1021/nn501896e.

[31] B. Gotsmann, M.A. Lantz, Atomistic wear in a single asperity sliding contact, Phys. Rev. Lett. 101 (2008) 125501. https://doi.org/10.1103/PhysRevLett.101.125501.

[32] N.S. Park, M.W. Kim, S.C. Langford, J.T. Dickinson, Atomic layer wear of single-crystal calcite in aqueous solution using scanning force microscopy, J. Appl. Phys. 80 (1996) 2680-2686. https://doi.org/10.1063/1.363185.

[33] P.E. Sheehan, The wear kinetics of NaCl under dry nitrogen and at low humidities, Chem. Phys. Lett. 410 (2005) 151-155. https://doi.org/10.1016/j.cplett.2005.05.060.

[34] S. Peeters, P. Restuccia, S. Loehlé, B. Thiebaut, M.C. Righi, Tribochemical Reactions of MoDTC Lubricant Additives with Iron by Quantum Mechanics/Molecular Mechanics Simulations, J. Phys. Chem. C. 124 (2020) 13688-13694. https://doi.org/10.1021/acs.jpcc.0c02211.

[35] M.C. Righi, S. Loehlé, M.I. De Barros Bouchet, D. Philippon, J.M. Martin, Trimethyl-phosphite dissociative adsorption on iron by combined first-principle calculations and XPS experiments, RSC Adv. 5 (2015) 101162-101168. https://doi.org/10.1039/c5ra14446a.

[36] S. Loehlé, M.C. Righi, First principles study of organophosphorus additives in boundary lubrication conditions: Effects of hydrocarbon chain length, Lubr. Sci. 29 (2017) 485–491. https://doi.org/10.1002/ls.1382.

[37] E. Osei-Agyemang, S. Berkebile, A. Martini, Decomposition mechanisms of anti-wear lubricant additive tricresyl phosphate on iron surfaces using DFT and atomistic thermodynamic studies, Tribol. Lett. 66 (2018) 1–22. https://doi.org/10.1007/s11249-018-0998-x.

[38] Tom Bettens, Mercedes Alonso, Paul Geerlings, F.D. Proft, Implementing the mechanical force into the conceptual DFT framework: understanding and predicting molecular mechanochemical properties, Phys. Chem. Chem. Phys. 21 (2019) 7378–7388. https://doi.org/10.1039/C8CP07349J.

[39] Z. Li, I. Szlufarska, Physical Origin of the Mechanochemical Coupling at Interfaces, Phys. Rev. Lett. 7 (2021) 076001. https://doi.org/10.1103/PhysRevLett.126.076001.

[40] T.P. Senftle, S. Hong, M.M. Islam, S.B. Kylasa, Y. Zheng, Y.K. Shin, C. Junkermeier, R. Engel-Herbert, M.J. Janik, H.M. Aktulga, T. Verstraelen, A. Grama, A.C.T. van Duin, The ReaxFF reactive force-field: development, applications and future directions, npj Comput. Mater. 2016 21. 2 (2016) 1–14. https://doi.org/10.1038/npjcompumats.2015.11.

[41] A. Martini, S.J. Eder, N. Dörr, Tribochemistry: A Review of Reactive Molecular Dynamics Simulations, Lubr. 8 (2020) 44. https://doi.org/10.3390/LUBRICANTS8040044.

[42] J. Wen, T. Ma, W. Zhang, G. Psofogiannakis, A.C.T. van Duin, L. Chen, L. Qian, Y. Hu, X. Lu, Atomic insight into tribochemical wear mechanism of silicon at the Si/SiO2 interface in aqueous environment: Molecular dynamics simulations using ReaxFF reactive force field, Appl. Surf. Sci. 390 (2016) 216–223. https://doi.org/10.1016/J.APSUSC.2016.08.082.

[43] D. Yue, T. Ma, Y. Hu, J. Yeon, A.C.T. Van Duin, H. Wang, J. Luo, Tribochemical Mechanism of Amorphous Silica Asperities in Aqueous Environment: A Reactive Molecular Dynamics Study, Langmuir 31 (2015): 1429-1436. https://doi.org/10.1021/la5042663.

[44] J. Wen, T. Ma, W. Zhang, A.C.T. van Duin, X. Lu, Atomistic mechanisms of Si chemical mechanical polishing in aqueous H2O2: ReaxFF reactive molecular dynamics simulations, Comput. Mater. Sci. 131 (2017) 230–238. https://doi.org/10.1016/J.COMMATSCI.2017.02.005.

[45] S.H. Hahn, S.H. Kim, Atomistic understanding of surface wear process of sodium silicate glass in dry versus humid environments, 103 (2020) 3060–3069. https://doi.org/10.1111/jace.17008.

[46] H. He, S.H. Hahn, J. Yu, Q. Qiao, A.C.T. van Duin, S.H. Kim, Friction-induced subsurface densification of glass at contact stress far below indentation damage threshold, Acta Mater. 189 (2020) 166–173. https://doi.org/10.1016/J.ACTAMAT.2020.03.005.

[47] C. Ayestarán Latorre, J.E. Remias, J.D. Moore, H.A. Spikes, D. Dini, J.P. Ewen, Mechanochemistry of Phosphate Esters Confined between Sliding Iron Surfaces, Commun. Chem. 4 (2021) 1-11. https://doi.org/10.1038/s42004-021-00615-x

[48] K. Mohammadtabar, S.J. Eder, P.O. Bedolla, N. Do, A. Martini, Reactive Molecular Dynamics Simulations of Thermal Film Growth from di-tert-butyl disulfide on an Fe (100) surface, Langmuir. 34 (2018) 15681-15688. https://doi.org/10.1021/acs.langmuir.8b03170.

[49] K. Mohammadtabar, S.J. Eder, N. Do, A. Martini, Heat-, Load-, and Shear-driven Reactions of di-tert-butyl disulfide on Fe (100), J. Phys. Chem. C. 123 (2019) 19688-19692. https://doi.org/10.1021/acs.jpcc.9b05068.

[50] A. Martini, A. Khajeh, F.H. Bhuiyan, J.E. Mogonye, R.A. Pesce-Rodriguez, S. Berkebile, Thermal decomposition of tricresyl phosphate on ferrous surfaces, J. Phys. Chem. C. 125 (2021) 5076-5087. https://doi.org/10.1021/acs.jpcc.0c10789.

[51] X. He, A.J. Barthel, S.H. Kim, Tribochemical synthesis of nano-lubricant films from adsorbed molecules at sliding solid interface: Tribo-polymers from α-pinene, pinane, and n-decane, Surf. Sci. 648 (2016) 352-359. https://doi.org/10.1016/j.susc.2016.01.005.

[52] A.C. Chipara, T. Tsafack, P.S. Owuor, J. Yeon, C.E. Junkermeier, A.C.T. van Duin, S. Bhowmick, S.A.S. Asif, S. Radhakrishnan, J.H. Park, G. Brunetto, B.A. Kaipparettu, D.S. Galvão, M. Chipara, J. Lou, H.H. Tsang, M. Dubey, R. Vajtai, C.S. Tiwary, P.M. Ajayan, Underwater adhesive using solid–liquid polymer mixes, Mater. Today Chem. 9 (2018) 149-157. https://doi.org/10.1016/j.mtchem.2018.07.002.

[53] S.G. Srinivasan, A.C.T. van Duin, Molecular-Dynamics-Based Study of the Collisions of Hyperthermal Atomic Oxygen with Graphene Using the ReaxFF Reactive Force Field, J. Phys. Chem. A. 115 (2011) 13269–13280. https://doi.org/10.1021/JP207179X.

[54] Kimberly Chenoweth, and Adri C. T. van Duin, I. William A. Goddard, ReaxFF Reactive Force Field for Molecular Dynamics Simulations of Hydrocarbon Oxidation, J. Phys. Chem. A. 112 (2008) 1040–1053. https://doi.org/10.1021/JP709896W.

[55] Kimberly Chenoweth, Sam Cheung, Adri C. T. van Duin, William A. Goddard, E.M. Kober, Simulations on the Thermal Decomposition of a Poly (dimethylsiloxane) Polymer Using the ReaxFF Reactive Force Field, J. Am. Chem. Soc. 127 (2005) 7192–7202. https://doi.org/10.1021/JA050980T.

[56] S. Plimpton, Fast Parallel Algorithms for Short-Range Molecular Dynamics, J. Comput. Phys. 117 (1995) 1–19. https://doi.org/10.1006/JCPH.1995.1039.

[57] A. Stukowski, Visualization and Analysis of Atomistic Simulation Data with OVITO–the Open Visualization Tool, Model. Simul. Mater. Sci. Eng. 18 (2009) 015012. https://doi.org/10.1088/0965-0393/18/1/015012.

[58] X. He, A. Pollock, S.H. Kim, Effect of gas environment on mechanochemical reaction: A model study with tribo-polymerization of α-pinene in inert, oxidative, and reductive gases, Tribology Letters. 67 (2019) 1–9. doi:10.1007/s11249-019-1136-0.

[59] X. He, D. Ngo, S.H. Kim, Mechanochemical reactions of adsorbates at tribological interfaces: Tribopolymerizations of allyl alcohol coadsorbed with water on silicon oxide, Langmuir. 35 (2019) 15451–15458. doi:10.1021/acs.langmuir.9b01663.

[60] J.L. Howard, Q. Cao, D.L. Browne, Mechanochemistry as an Emerging Tool for Molecular Synthesis: What can it offer?, Chem. Sci. 9 (2018) 3080–3094. https://doi.org/10.1039/c7sc05371a.

[61] J. Andersen, J. Mack, Mechanochemistry and Organic Synthesis: From Mystical to Practical, Green Chem. 20 (2018) 1435–1443. https://doi.org/10.1039/C7GC03797J.

[62] M. Menzinger, R. Wolfgang, The Meaning and Use of the Arrhenius Activation Energy, Angew. Chemie Int. Ed. English. 8 (1969) 438–444. https://doi.org/10.1002/ANIE.196904381.